Assessing dynamic vegetation model parameter uncertainty across Alaskan arctic tundra plant communities

EUGÉNIE S. EUSKIRCHEN [iD],[1,5] SHAWN P. SERBIN [iD],[2] TOBEY B. CARMAN,[1] JENNIFER M. FRATERRIGO [iD],[3] HÉLÈNE GENET [iD],[1] COLLEEN M. IVERSEN [iD],[4] VERITY SALMON [iD],[4] AND A. DAVID MCGUIRE [iD][1]

[1]*Institute of Arctic Biology, University of Alaska Fairbanks, Fairbanks, Alaska 99775 USA*
[2]*Terrestrial Ecosystem Science & Technology Group, Environmental Sciences Department, Brookhaven National Laboratory, Upton, New York 11973 USA*
[3]*Department of Natural Resources and Environmental Sciences, University of Illinois at Urbana-Champaign, Urbana, Illinois 61801 USA*
[4]*Environmental Sciences Division and Climate Change Science Institute, Oak Ridge National Laboratory, Oak Ridge, Tennessee 37831 USA*

Abstract. As the Arctic region moves into uncharted territory under a warming climate, it is important to refine the terrestrial biosphere models (TBMs) that help us understand and predict change. One fundamental uncertainty in TBMs relates to model parameters, configuration variables internal to the model whose value can be estimated from data. We incorporate a version of the Terrestrial Ecosystem Model (TEM) developed for arctic ecosystems into the Predictive Ecosystem Analyzer (PEcAn) framework. PEcAn treats model parameters as probability distributions, estimates parameters based on a synthesis of available field data, and then quantifies both model sensitivity and uncertainty to a given parameter or suite of parameters. We examined how variation in 21 parameters in the equation for gross primary production influenced model sensitivity and uncertainty in terms of two carbon fluxes (net primary productivity and heterotrophic respiration) and two carbon (C) pools (vegetation C and soil C). We set up different parameterizations of TEM across a range of tundra types (tussock tundra, heath tundra, wet sedge tundra, and shrub tundra) in northern Alaska, along a latitudinal transect extending from the coastal plain near Utqiaġvik to the southern foothills of the Brooks Range, to the Seward Peninsula. TEM was most sensitive to parameters related to the temperature regulation of photosynthesis. Model uncertainty was mostly due to parameters related to leaf area, temperature regulation of photosynthesis, and the stomatal responses to ambient light conditions. Our analysis also showed that sensitivity and uncertainty to a given parameter varied spatially. At some sites, model sensitivity and uncertainty tended to be connected to a wider range of parameters, underlining the importance of assessing tundra community processes across environmental gradients or geographic locations. Generally, across sites, the flux of net primary productivity (NPP) and pool of vegetation C had about equal uncertainty, while heterotrophic respiration had higher uncertainty than the pool of soil C. Our study illustrates the complexity inherent in evaluating parameter uncertainty across highly heterogeneous arctic tundra plant communities. It also provides a framework for iteratively testing how newly collected field data related to key parameters may result in more effective forecasting of Arctic change.

Key words: arctic carbon budget; arctic tundra; landscape heterogeneity; model uncertainty; parameter sensitivity; terrestrial biosphere model.

INTRODUCTION

In arctic terrestrial ecosystems, climate is the most important driver of change. As the Arctic warms at twice the rate relative to the rest of the globe, with some regions experiencing even faster rates, tundra ecosystems are undergoing unprecedented change (Box et al. 2019, Overland et al. 2019). This warming and related lengthening of the Arctic growing season by ~2.5 days per decade (Euskirchen et al. 2006, Park et al. 2016) is increasing tundra plant carbon (C) uptake and vegetation productivity, with a distinct impact on the growth of woody shrub vegetation (Sturm et al. 2001, Myers-Smith et al. 2011, 2015, Keenan and Riley 2018). However, these increases in vegetation productivity are not uniform, with many areas remaining stable or even

showing declining productivity (Bhatt et al. 2013, Phoenix and Bjerke 2016, Lara et al. 2018). Together with vegetation impacts, warming in northern high latitudes is thickening the active layer (a soil layer above permafrost that freezes and thaws seasonally). This thickening of the active layer makes available for decomposition and release the large amounts of organic C (Hugelius et al. 2014, Strauss et al. 2017) that have been stored in these cold permafrost soils for millennia (Schuur et al. 2015), and may result in the release of potent greenhouse gases and a positive feedback to warming. However, it is unclear if these soil C losses will be counterbalanced by increased plant C uptake (McGuire et al. 2018, Mekonnen et al. 2018).

As the Arctic region moves into uncharted territory, it is important to refine the terrestrial biosphere models (TBMs) that help us to further understand and predict these changes. These models include several sources of uncertainty, including uncertainty in how best to represent the complexity of the system (Bradford et al. 2016, Lique et al. 2016, Lovenduski and Bonan 2017, López-Blanco et al. 2018), driving climate and atmospheric data (Clein et al. 2007, Cowtan and Way 2014, Dodd et al. 2015), validation data (including both a lack of validation data and uncertainty associated with such measurements; Lovenduski and Bonan 2017, Fisher et al. 2018), and model parameters (Hararuk et al. 2015, Fisher et al. 2018). A model parameter is a configuration variable internal to the model and whose value can be estimated from data collected in the field or determined through empirical experimental approaches in a laboratory setting. Model parameter uncertainty depends upon (1) the sensitivity of the model to the input parameters (i.e., the change in model output resulting from a change in parameter value) and (2) the uncertainty of these parameters. A sensitive parameter that is well constrained by observations may have a lower impact on model uncertainty than a moderately sensitive parameter that is poorly constrained.

Terrestrial biosphere models are often characterized by a high level of complexity, resulting in the need for a large number of model parameters. Even when the model outputs and observations agree, it remains important to address overall parameter uncertainty (i.e., confront the estimated parameter value with the range of possible variation from observations), to confirm this agreement is for the correct reasons. However, it is challenging to determine the influence model parameter uncertainty has on model results. This is, in large part, due to the complex nature of this endeavor, with dozens of model input parameters that can vary over space and time, and evaluating alternative parameter combinations can have many complex interconnected feedbacks in the model (Viskari et al. 2019). Furthermore, while some parameters can be well constrained by a rich source of data, a number of them are often poorly documented, especially for remote high latitude regions where observations are scarce (Schimel et al. 2015) and the tundra

vegetation communities display large amounts of heterogeneity across the landscape. Hence, it was parameters such as these, with little to no field data, which motivated the determination of how these parameters influence model outputs. That is, would the extra effort required to measure these parameters in the field pay off in terms of reducing model uncertainty?

Evaluation of ecosystem model parameter uncertainty requires an efficient methodology to test the model parameterizations of the underlying plants and soils in a given ecosystem and to iteratively test a model parameterization with new data. One such framework for this evaluation is the Predictive Ecosystem Analyzer (PEcAn, Fig. 1; Dietze et al. 2013, LeBauer et al. 2013, Wang et al. 2013). PEcAn is an ecoinformatics toolbox that consists of a scientific workflow to manage environmental data and a Bayesian data assimilation system to synthesize this information within ecosystem models. PEcAn treats model parameters as probability distributions and estimates parameters based on synthesis of available field data, and then quantifies both parameter and model output uncertainty. While PEcAn has been applied broadly across ecosystems and biomes and can interface with a wide range of ecosystem models, it has not been used specifically in a study that focuses on the various tundra types that comprise arctic terrestrial ecosystems. Here, we incorporate the Terrestrial Ecosystem Model with Dynamic Vegetation and Dynamic Organic Soil Layers (DVM-DOS-TEM, v0.3.0, referred hereafter as simply TEM) into the PEcAn framework. TEM has been developed for and applied to high-latitude arctic tundra and boreal ecosystems and has been shown to have generally good agreement with field data from these regions (Euskirchen et al. 2009, 2014, Genet et al. 2018). To date, the overall parameter uncertainty in the model has not yet been directly accessed.

Furthermore, recent data collection efforts at an array of sites across northern Alaska (Fig. 2) provides motivation to assess parameter measurement needs and run model simulations at these specific locations.

Across four dominant types of arctic tundra communities (heath tundra, shrub tundra, tussock tundra, and wet sedge tundra) and the plant functional types (PFTs) within each community (e.g., deciduous shrubs, evergreen shrubs, mosses, lichens), we pose the following questions:

1) Based on a set of 21 selected parameters that control C fluxes and pools, to which parameters is the model most sensitive and which parameters result in the greatest model uncertainty?
2) How does this sensitivity and uncertainty vary across output variables, including those pertaining to vegetation and soil C pools and fluxes in arctic tundra?
3) What is the effect of site location and vegetation composition on sensitivity and model uncertainty, e.g., is shrub tundra in the Seward Peninsula characterized by a different set of key sensitivity and
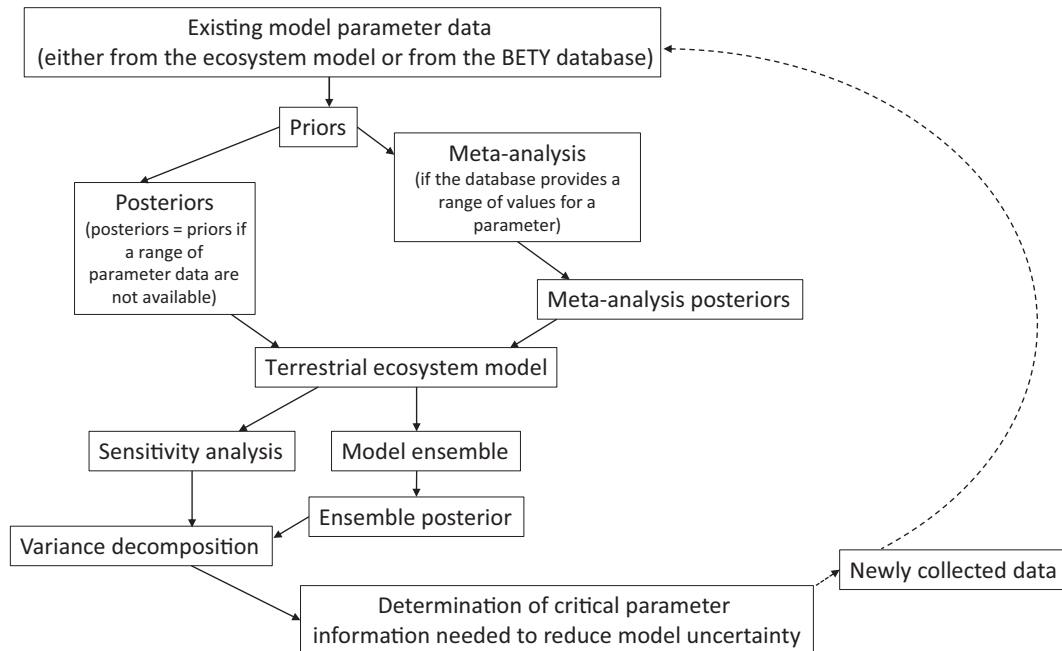
Fig. 1. Diagram of the workflow of the Predictive Ecosystem Analyzer (PEcAn) coupled with the Terrestrial Ecosystem Model (TEM). Initially, the BETY database is queried for information related to parameters in TEM for a given plant functional type. If available, these data are synthesized in a meta-analysis, resulting in a posterior trait distribution. In our case, data were available for one parameter, leaf area index (LAI). For the remaining parameters, the posteriors are equivalent to the priors, with the distribution chosen to best represent a given parameter. The ensemble of model runs with the TEM-PEcAn framework produces the posterior distribution of model outputs, representing a probabilistic assessment or forecast that accounts for parameter uncertainty. The sensitivity analysis and variance decomposition are then calculated, providing insight to the relative contribution of each parameter, and how to collect future data to reduce model parameter uncertainty.

uncertainty parameters than a shrub tundra site in the foothills of the Brooks Range? Are patterns in model sensitivity and parameter uncertainty shared across a range of tundra types that are in close proximity?

METHODS

Simulation sites

To gain a better understanding of model sensitivity and uncertainty across a range of arctic tundra plant communities, we performed model simulations across Arctic Alaska that represent (1) the coastal floodplain in northern Alaska, (2) a latitudinal transect extending from the southern to northern foothills of the Brooks Range paralleling the Dalton Highway in northeastern Alaska, and (3) Beringian Alaska in the Seward Peninsula. These sites span two bioclimates, Subzones C and E (Fig. 2, Table 1; Walker et al. 2005). The site in the coastal floodplain is in the northern most of these bioclimates, Subzone C, and comprises wet sedge tundra near Utqiaġvik, Alaska. The Dalton Highway latitudinal transect in northeastern Alaska spans Subzone E, and comprises sites in low shrub tundra (sites abbreviated as DHS1–DHS5 later on). In Beringian Alaska, our simulations include

sites in heath tundra, moist acidic tussock tundra, and low shrub tundra in Subzone E, located in close proximity to one another on a hillslope (<1 km apart, and consequently all under the same climate forcing) and approximately 100 km north of the town of Nome, Alaska in the Seward Peninsula (sites named Kougarok later on). We examine the spatial variability of model sensitivity and uncertainty across the various sites, including by comparing results for low shrub tundra from the latitudinal transect and the shrub tundra at the Kougarok site. We examine the differences in model sensitivity and uncertainty between vegetation communities by comparing results from the Kougarok site for shrub, tussock, and heath tundra, and the Utqiagvik site for wet sedge. Each of these sites has been the focus of field studies in recent years (Langford et al. 2016, 2019, Norby et al. 2019, Salmon et al. 2019, Chen et al. 2020). Thus, we selected to perform our simulations at these sites because, in future studies, field data collected at these sites may be incorporated into our model parameterizations (data collection was still ongoing during our development of this study), and additional field data for model parameterization and evaluation that we find lacking based on the study presented here could then be collected at these sites.
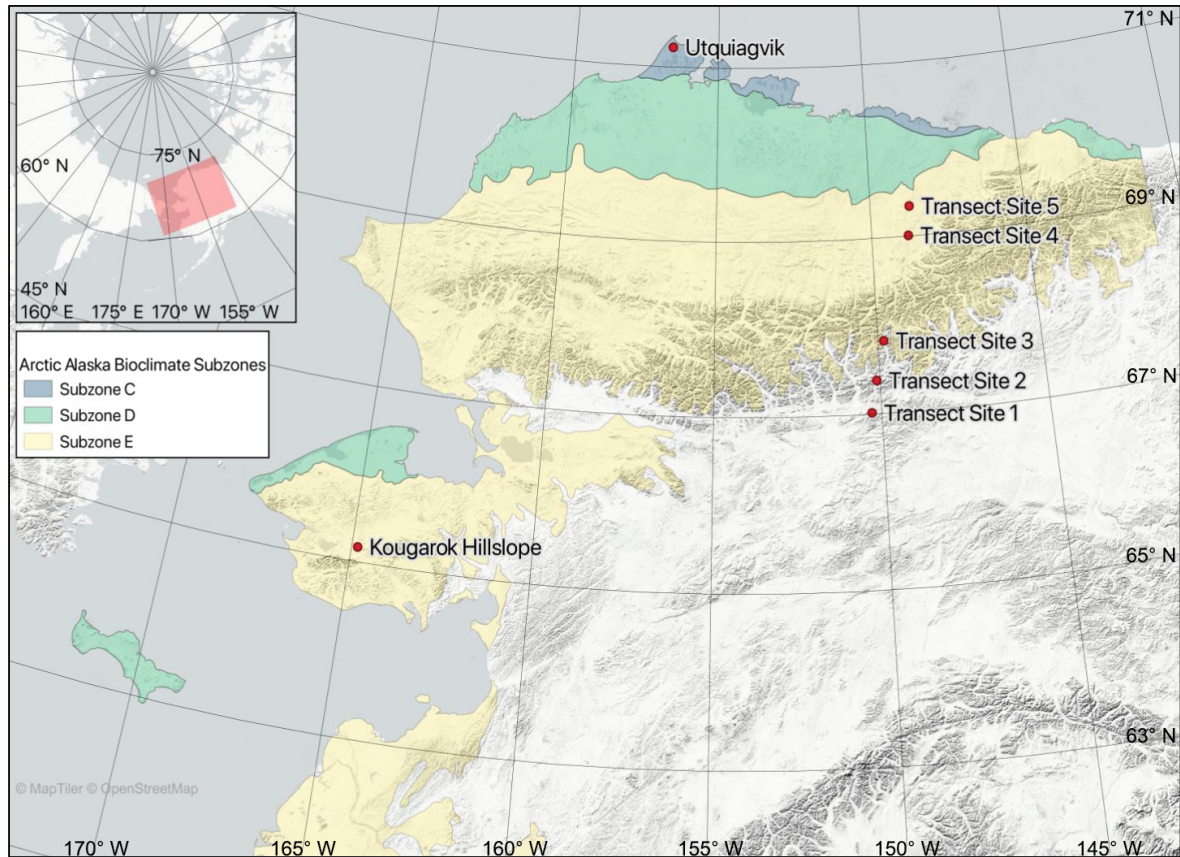
Fig. 2. Simulation sites used in this study and their bioclimatic subzones in Alaska. The subzones can be represented through their mean July temperatures, with warmer July temperatures increasing the size, horizontal cover, abundance, productivity, and variety of plants. In Alaska, woody plants occur as hemiprostrate dwarf shrubs (<15 cm tall) in Subzone C (mean July temperatures about 5°–7°C), erect dwarf shrubs (<40 cm tall) in Subzone D (mean July temperature about 7°–9°C), and low shrubs (40–200 cm tall) in Subzone E (mean July temperature about 9°–12°C).

Overview of DVM-DOS-TEM

We incorporated the Terrestrial Ecosystem Model with Dynamic Vegetation and Dynamic Organic Soil Layers (DVM-DOS-TEM, or simply TEM) into the Predictive Ecosystem Analyzer (PEcAn) framework (Fig. 2). The dynamic vegetation component of TEM has been described previously (Euskirchen et al. 2009, 2014) as has the dynamic organic soil layer version of TEM (Yi et al. 2010, Euskirchen et al. 2016, Genet et al. 2018). TEM has been used extensively in arctic and boreal permafrost regions with applications to the soil environment (Zhuang et al. 2001, 2003, Yi et al. 2010), tundra vegetation dynamics (Euskirchen et al. 2009, 2014), carbon storage (Genet et al. 2018), and feedbacks to climate (Euskirchen et al. 2007, 2016). We briefly describe the model here.

TEM is a process-based ecosystem model that is designed to simulate carbon (C) and nitrogen (N) pools of the vegetation and the soil, and carbon and nitrogen fluxes among vegetation, soil, and the atmosphere (Raich et al. 1991, McGuire et al. 1992). The version of TEM used in this study (DVM-DOS-TEM v0.3.0, *available online*)[6] comprises four modules: an environmental module, a dynamic organic soil module, a disturbance module, and an ecological module with vegetation dynamics. The environmental module simulates the dynamics of biophysical processes in the soil and the atmosphere, and includes soil temperature, freeze/thaw fronts (including permafrost dynamics), water table and soil moisture conditions for multiple layers within the moss, fibric and humic organic horizons, and mineral soil horizons. The dynamic organic soil layer module calculates thickness of the fibric and the humic organic layers and incorporates changes in the thickness of these layers due to ecological processes (litterfall, decomposition, and burial) as well as fire disturbance. The disturbance module simulates the effects of logging and wildfire on soil and vegetation C and N pools and is not applied to the tundra sites simulated in this study. The ecological module simulates carbon and nitrogen dynamics in the atmosphere, vegetation, and soil,

---

[6] http://github.com/ua-snap/dvm-dos-tem

Table 1. Tundra community types and the four plant functional types (PFTs) within each tundra community that had the four greatest initial values for vegetation carbon (C) stocks (e.g., biomass) among the PFTs that comprised each community, with that percentage of vegetation C provided next to each PFT.

Tundra community type, PFTs, and site	MAAT (°C)	P (cm)
Heath		
Decidous shrubs (21%), evergreen shrubs (49%), mosses (28%), lichens (2%)		
Kougarok (65.167° N, 164.833° W)	−3.5	41
Shrub		
Dwarf birch (58%), willow (22%), other deciduous shrubs (5%), feathermoss (9%)		
Kougarok (65.167° N, 164.833° W)	−3.5	41
DHS1 (67.017° N, −150.293° W)	−6.7	38
DHS2 (67.383° N, −150.101° W)	−6.2	25
DHS3 (67.828° N, −149.821° W)	−7.6	21
DHS4 (69.009° N, −148.825° W)	−9.1	16
DHS5 (69.343° N, −148.728° W)	−9.6	16
Tussock		
Dwarf birch (10%), evergreen shrubs (27%), sedges (34%), *Sphagnum* (11%)		
Kougarok (65.167° N, 164.833° W)	−3.5	41
Wet sedge		
Sedges (72%), grasses (2%), feathermoss (8%), *Sphagnum* (8%)		
Utqiaġvik (71.228° N, −156.602° W)	−11.1	16

Notes: "Sites" refers to the site name and latitude and longitude where each tundra community type was simulated. Mean annual air temperature (MAAT, °C) and total annual precipitation (P, mm) are given for the years 1990–2015, as calculated with the model input data from the Climate Research Unit (see *Methods*).

including the vegetation dynamics of the ecosystems. The dynamic organic soil layer module is linked to the ecological module so that the thickness of the organic layers is linked to the amount of carbon stored. Each plant community type in TEM (e.g., heath tundra, shrub tundra, tussock tundra, wet sedge tundra) is composed of up to 10 plant functional types (PFTs) that are parameterized differently depending on the community in which they are found. Example PFTs are dwarf birch shrubs, willow shrubs, other deciduous shrubs, evergreen shrubs, grasses, sedges, forbs, lichens, feathermoss, and *Sphagnum* moss. The PFTs in each community type compete for water, light, and available nitrogen. Over the course of a model simulation, a given PFT may show increases or decreases in biomass, depending on its ability to compete and in response to changing environmental conditions. Typically, under a warming arctic climate, our model has simulated increases in biomass across all PFTs, although shorter-stature PFTs have been shown to exhibit slight declines in some instances due to lower light availability as shrubs grow larger (Euskirchen et al. 2009, 2016).

The driving inputs for TEM are the climate variables including monthly mean air temperature, total monthly precipitation, net incoming shortwave radiation, and vapor pressure (Climate Research Unit—CRU TS 3.1; Harris et al. 2014, and downscaled as described in Euskirchen et al. 2016) as well as yearly atmospheric CO_2 concentration. Site drainage classification, soil texture classification, elevation, and vegetation community type are used to initialize model simulations. The model is calibrated once for a representative field site for each vegetation community type using rate-limiting parameters represented in the model based on target values of C and N pools and fluxes of representative tundra ecosystems. This calibration procedure is performed because these rate-limiting parameters typically cannot be determined directly from available data or published information. In the calibration process, rate-limiting parameters for GPP (C_{max} in Eq. 1 below), autotrophic respiration (K_r), heterotrophic respiration (K_d), maximum plant N uptake (N_{max}), N in litter production, and soil N immobilization are adjusted until model values match the field-based estimates of GPP, NPP, N uptake, and vegetation and soil C and N pools at the calibration site. These adjusted rate-limiting parameters and field-based estimates of GPP, NPP, N uptake, and vegetation and soil C and N pools are then used to initialize the model simulations when the model is simulated at other sites. Further information on the calibration process is also provided in previous publications that apply TEM to simulate ecosystem dynamics (Raich et al. 1991, McGuire et al. 1992, Euskirchen et al. 2009, 2014).

Description of TEM parameters evaluated in the PEcAn framework

We evaluated 21 model parameters used in TEM (Table 2) within the PEcAn framework, representing a broad suite of ecological processes in TEM. None of these 21 parameters are included in the calibration procedure described above. Each parameter we evaluated relates to the key equation in the model (Eq. 1), which governs gross primary production (GPP). In TEM, the overall amount of GPP of a plant functional type (GPP_{PFT}) within a given tundra community, is regulated by the maximum rate of C assimilation (C_{max}), moderated by several functions, and is calculated for each leaf, wood (including woody course roots), and fine root component of a PFT

$$GPP_{PFT} = f(CO_2)f(PAR)f(T)f(G_v)(LEAF)_{max} \times f(FOLIAGE)f(THAWPCT)f(N_{AV})$$ (1)

where $f(CO_2)$ is a function of the atmospheric CO_2 concentration, $f(PAR)$ is a function of photosynthetically active radiation, $f(T)$ is a function of the monthly mean air temperature, $f(G_v)$ is a function of relative conductance of the vegetation to CO_2 uptake (G_v), $f(LEAF)$ is

TABLE 2. Description of parameters used with the simulation and summary of the prior distributions and range (when applicable) of parameter medians or range of medians across PFTs, grouped according to their ecological function.

Parameter (units)	Description and reference for parameter values	Distribution	Range of a statistic across PFTs				
			Medians	a	b	LCL	UCL
Parameters related to photosynthetic temperature (**Photo temp**)							
T_{min} (°C)	minimum temperature for photosynthesis	Uniform	−7.9 to −4.9	−7.5 to −11.0	−5.0 to 0	−7.4 to −10.8	−0.25 to −5.1
T_{optmin} (°C)	the range of minimal temperatures for photosynthesis	Uniform	3.5–5.5	1.5–2.0	9.0–9.5	1.7–2.2	8.8–9.3
T_{optmax} (°C)	the range of maximum temperatures for photosynthesis	Uniform	20.0–23.0	10.0–20.0	25.0–30.0	10.5–20.5	24.7–29.5
T_{max} (°C)	maximum temperature for photosynthesis	Uniform	25.0–35.0	20.0–22.0	28.0–45.0	20.2–25.5	27.8–44.5
Parameters related to leaf area (**Leaf area**)							
SLA (m^2/kg leaf)	specific leaf area (leaf area per leaf mass)	Weibull	12.8	3.5	14.2	4.8	20.7
iLAI (m^2/m^2)	starting value for leaf area index	Gamma	0.035–2.0	1.0–2.0	0.25–20.0	0.001–1.51	0.18–2.5
Parameters related to fine roots (**Fine roots**)							
Fine root productivity at depth [10]–[50] (%)	fine root allocation vertically in soils, every 10 cm from 0 to 50 cm (%); not applicable for all PFTs (a total of five parameters)	Uniform	2.0–50.0	0.01–35	4.0–90.0	0.11–35.5	3.9–88.0
Parameters related to leaf stomata conductance and vpd (**Leaf cond**)							
Vpd_open (Pa)	vpd for leaf stomata fully opened	Uniform	0.9	0.8	1.1	0.8	1.1
Vpd_closed (Pa)	vpd for leaf stomata fully closed	Uniform	4.1	3.2	5.0	3.3	5.0
Cuticular conductance (μmol·m^{-2}·s^{-1})	cuticular conductance of a leaf	Log-normal	3,006.5	8.0	0.7	778.1	11,766.1
Parameter related to radiation influence on leaf stomates (**PPFD50**)							
PPFD50 (μmol·m^{-2}·s^{-1})	amount of photosynthetically active radiation at which stomates partially (half) close	Uniform	75.0	5	145	8.6	141.5
Parameter related to canopy conductance (**Canopy cond**)							
Gcmax (m/s)	maximum canopy conductance	Uniform	0.003	0.003	0.004	0.003	0.004
Parameter related to nitrogen availability (**Labile N**)							
Labile N (g N/m^2)	labile N concentration	Uniform	0.20	0.05	0.34	0.15	0.34
Parameter related to reflectivity (**Albedo**)							
Albedo (W/m^2)	shortwave albedo	Uniform	0.16	0.01	0.30	0.02	0.29
Parameters related to light competition (**Extin coeff**)							
Extinction coefficient	light extinction coefficient for light competition across PFTs	Gamma	0.37–0.47	4.0–5.0	0.40–10.0	0.15–0.16	0.55–1.02
kLAI	extinction coefficient for converting between LAI and foliar percent cover	Uniform	0.25–0.45	0.01–0.30	0.34–0.60	0.03–0.31	0.33–0.63

Notes: Prior distributions are used in the meta-analysis for one parameter, specific leaf area (SLA), and for all other parameters the priors were equal to the posterior distributions (as described in *Methods*). Terms *a* and *b* are the first and second parameters of the probability distribution. LCL and UCL are the upper and lower 95% credible limits, respectively. LAI, leaf area index; vpd, vapor pressure deficit. Parenthetical documentation in boldface type along with each parameter grouping refers to the abbreviation of the parameter grouping used in figure legends and elsewhere in the manuscript. The full table of values for each community type, PFT, and parameter is available through our code repository, https://zenodo.org/record/4349004.

monthly leaf area relative to leaf area during the month of maximum leaf area, f(FOLIAGE) is a scalar function that ranges from 0.0 to 1.0 and represents the ratio of canopy leaf biomass relative to maximum leaf biomass, f(THAWPCT) is a freeze–thaw index that calculates the proportion of the month that the rooting zone of the soil is either frozen or thawed using simulated soil temperatures at 10 cm depth (used to represent the onset of photosynthesis), and $f(N_{AV})$ is dynamically calculated to model the limiting effects of plant N status on GPP based on a comparison of N availability and N requirement.

Each of the parameters we chose to examine within the PEcAn framework are directly or indirectly related to the functions within the GPP_{PFT} equation. We describe here how the parameters we chose to evaluate are generally related to the functions in Eq. 1. The f(PAR) function includes processes related to light availability, including the amount of photosynthetically active radiation at which stomates close halfway (PPFD50; Table 2). The $f(T)$ function includes a regulation of GPP by temperature constraints, including those related to optimal minimal and maximal temperatures for photosynthesis (pstemp_min, pstemp_low, pstemp_high, pstemp_max; Table 2, Appendix S1: Fig. S1; Tian et al. 1999). The functions f(LEAF) and f(FOLIAGE) govern the leaf area index (iLAI; Table 2) and specific leaf area (SLA) respectively, as impacted by water availability and season. The extinction coefficient for light competition, or light "harvesting" across PFTs (extin_coeff) and its scaling factor (kLAI) are also indirectly included in the f(FOLIAGE) function. Variables related to the influence of vapor pressure deficit (vpd) on canopy conductance (vpd_open, vpd_close; Table 2) are associated with the function for relative canopy conductance, $f(G_v)$, as is the maximum canopy conductance parameter (Gcmax) and cuticular conductance(gl_c). The allocation to fine roots and the vertical distribution of fine root biomass throughout the soil profile is based on fine-root biomass production coefficient for 10-cm vertical depth increments (frpod_perc 10–50; Table 2). These parameters are associated with the freeze–thaw index function f(THAW). The nitrogen supply is regulated by N availability and requirement, $f(N_{AV})$ above, including labile N availability (labileN, which changes over the course of the simulation, but is also initialized at the beginning of the simulation; Table 2). Some of these parameters, such as fine-root allocation at depth, are notoriously difficult to measure in the field and available field data are scarce, particularly for arctic tundra plant communities (Iversen et al. 2015).

PEcAn description and model simulations

The Predictive Ecosystem Analyzer (PEcAn, ver. 1.6.0) was developed to streamline the ecoinformatics of ecological models (LeBauer et al. 2013). PEcAn supports the flow of data used in such models, and aids in model parameterization, and error propagation, as well as uncertainty and sensitivity analysis. It can thus assist in evaluating what future data collection may help most to reduce model uncertainty for a given ecological model, or suite of ecological models.

In a typical model simulation, a model parameter is assigned a single value, typically based on the mean of a collection of field measurements. However, in PEcAn, available parameterization data can be assigned to a statistical distribution, called a "prior." Based on data available in the Biofuel Ecophysiological Traits and Yield database (BETY; *available online*),[7] the priors are synthesized using a Bayesian meta-analysis, resulting in a "posterior" distribution that summarizes the uncertainty associated with each parameter (LeBauer et al. 2013). Since the BETY database was initially developed with a focus on temperate ecosystems in the eastern and midwestern United States, the information in the database pertaining to tundra plants was minimal. In the application presented here, our posteriors were determined based on tundra plant data available in the BETY database for one parameter, specific leaf area (SLA), the one parameter for tundra plants available in the database that corresponded to a parameter in TEM. This posterior distribution is calculated using a linear mixed model for the unobserved "true" trait mean Θij, where i indexes the study site and j indexes each treatment within a study

$$\Theta ij = \beta_0 + \beta_{site}(i) + \beta_{tr|site}(ij) + \beta_{gh}I(i). \quad (2)$$

This equation includes the global trait mean (β_0), a normal random effect for the study site ($\beta_{site}(i)$, including spatial influences such as topography, soil, etc.), a nested normal random effect for any experimental treatments ($\beta_{tr|site}(ij)$, including the influence of temperature, N availability, etc.), and a fixed effect for greenhouse studies (β_{gh}; LeBauer et al. 2013, Raczka et al. 2018). The term $I(i)$ is an indicator variable set to 0 for field studies and 1 for studies conducted in a greenhouse, growth chamber or pot experiment. Additional details on the linear mixed model and the fitting procedure are found in LeBauer et al. (2013).

The remaining 20 parameters without tundra trait information available in the BETY database used the parameter information already specified in TEM. These are based on data collected for arctic tundra communities as part of the Arctic Long-Term Ecological Research (LTER) site near Toolik Field Station (Shaver and Chapin 1991, Van Wijk et al. 2003, Sullivan et al. 2007, Euskirchen et al. 2012, Gough et al. 2012, Sistla et al. 2013), and field studies on the Seward Peninsula (Thompson et al. 2004, 2006). These data are described previously in Euskirchen et al. (2009, 2016), and Genet et al. (2018), and summarized in Table 2. We formulated prior distributions for the central tendency

informed from this parameter information in TEM and used expert constraints on the confidence intervals (Table 2). Due to the lack of trait information in the database, the posterior distributions are then equivalent to the priors.

We then used PEcAn to propagate parameter uncertainty in TEM. PEcAn uses an ensemble-based Monte Carlo approach. An ensemble of model runs is a set of model runs that are parameterized by sampling from the trait parameter distributions. In our case, we chose 300 ensembles at each site for our suite of selected output variables because this number best represented the need to balance computationally expensive model run times with the need to complete analysis of the results. We performed the ensemble of model simulations for each site and each chosen PFT within that site, varying one PFT at a time, with the remaining PFTs left at their default parameters (Fig. 2, Table 1). For each ensemble member, parameter sets are sampled from the full joint parameter distribution of $\boldsymbol{\beta}_0$, the vector of all model parameters. Consequently, the model ensemble approximates the posterior distribution of the model output. This ensemble of model runs then results in a posterior distribution of the TEM output that is summarized with standard statistics (mean, standard deviation).

Each tundra community in TEM can be parameterized with up to 10 PFTs. In the analysis presented here, we chose to examine four of the PFTs within each tundra community that had the greatest initial values of vegetation carbon among the PFTs that comprised each community (i.e., biomass; Table 1). Given the computational requirements of running TEM within the PEcAn framework, we limited our simulations to the years 1990–2015. Our input climate data was based on that from the Climate Research Unit and downscaled to 1-km^2 resolution available through the Scenarios Network for Alaska + Arctic Planning (SNAP) data portal (*available online*).[8] We chose to examine four response variables, including two carbon fluxes and two carbon pools: the fluxes of net primary productivity (NPP) and heterotrophic respiration (R_H), and pools of soil carbon (Soil C) and vegetation carbon (Veg C).

Analysis: parameter uncertainty, model sensitivity, model uncertainty

Our analysis included three metrics of the model parameters. These included (1) the coefficient of variation (CV, %), (2) partial variance to quantify model uncertainty attributed to each parameter (%), and (3) elasticity (unitless) to quantify model sensitivity. We describe these metrics and associated calculations further below.

During the course of simulations, PEcAn evaluates each parameter at the posterior median and at the four posterior quantiles equivalent to $\pm[1, 2]\sigma$ quantiles of

[8] http://snap.uaf.edu/data

the parameter with all other parameters held at their nominal values (Table 2). The CV is calculated from the posterior parameter distributions, defined as the posterior standard deviation divided by the posterior mean.

The parameter uncertainty is transformed to the model uncertainty by fitting a cubic polynomial function (spline), g_p, to the modeled range of the output variable of interest (y-axis of the spline). The partial variance$_p$, or the fraction of the total variance contributed by parameter p (with x-axis of the spline being the range of values for a given parameter), quantifies this model uncertainty and is estimated as

$$\text{Partial variance}_p = \frac{\text{Var}[g_p(\beta_{\text{Op}})]}{\sum_{p=1}^{m}\text{Var}[g_p(\beta_{\text{Op}})]} \qquad (3)$$

where Var represents the variance operator, m is the total number of parameters that were varied, g_p is the fitted spline function, and β_{Op} is the Monte Carlo sample of the parameter values, based on the parameter distribution at which the spline is evaluated (LeBauer et al. 2013, Raczka et al. 2018). The partial variance calculation is a univariate approach and does not account for the interaction between parameters. The partial variance depends on the parameter uncertainty (CV) and the model sensitivity.

The sensitivity (unitless), often also referred to as "elasticity," is calculated as the derivative of g_p evaluated at the median parameter value, and then multiplied by the median parameter value ($\ddot{A}_p$) over the output median ($\bar{f}$)

$$\text{Sensitivity} = \frac{dg_p}{d\mathcal{O}_p} \times \frac{\mathcal{O}}{\bar{f}}. \qquad (4)$$

The sensitivity is thus a measure of how much a change in a parameter influences a model output. A model sensitivity of +1 means that a model output will double when a given parameter doubles, and conversely, a model sensitivity of −1 means that the model output is halved when a parameter doubles. In our analysis, we use the mean sensitivity and mean uncertainty across our 300 ensemble runs for each site and output variable.

Given the large number of parameters (21 parameters) and model ensemble simulations, we grouped the parameters into broad process themes: (1) temperature regulation of photosynthesis, (2) leaf functional traits related to leaf area, (3) fine-root depth distribution, (4) stomatal conductance, (5) the radiation influence on leaf stomates, (6) canopy conductance, (7) soil N availability, (8) albedo, and (9) light competition and light harvesting among PFTs (Table 2). We then took the mean sensitivity (after ensuring that the sensitivity values within a grouping were not opposite in sign, that is, positive and negative, between parameters) across a given parameter grouping to assess model sensitivity (elasticity), and the

sum the fraction of uncertainty (partial variance) to assess model uncertainty.

We examined the overall assessment of model sensitivity and uncertainty across arctic tundra plant communities (shrub, tussock, wet sedge, and heath tundra), the dominant plant functional types within them (Table 1), and four output variables (NPP, R_H, Soil C, Vegetation C). Therefore, there were 144 estimates each for sensitivity and uncertainty for each of the 21 parameters based on the parameter groupings in Table 2, except for the fine-root parameters where there were 100 estimates each for sensitivity and uncertainty since the non-vascular mosses and lichens do not have fine roots. Following these general summaries of sensitivity and uncertainty, we then examined the spatial variability of model uncertainty by comparing results from the shrub tundra transect (DHS1–DHS5) and the shrub tundra at the Kougarok site. We examined differences among community by comparing model uncertainty for the three tundra types located within close proximity at the Kougarok site, and the wet sedge tundra in Utqiagvik.

RESULTS

Parameter coefficient of variation

We summarized the parameter coefficient of variation (CV) by computing the mean and standard deviation of the CV of the posterior distribution of the parameter groupings across the plant functional types in the four tundra plant communities (i.e., without aggregating across PFTs or communities prior to calculating the mean and standard deviation of the CV; Fig. 3). The mean CV of the albedo, fine roots, labile soil N, leaf conductance, and the radiation influence on leaf stomates (PPFD50) parameter groupings were all roughly ~0.5. The mean CV of the canopy conductance (0.1) and
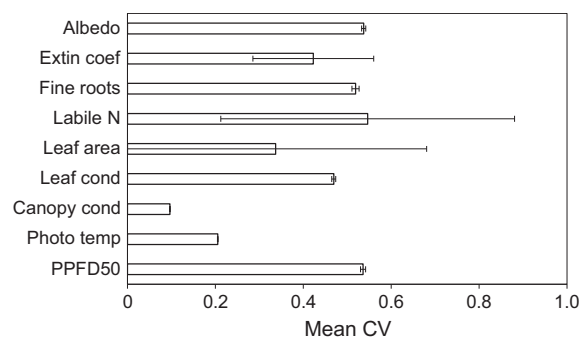

FIG. 3. Parameter uncertainty represented as the mean (error bars represent the standard deviation) of the coefficient of variation (CV). The mean and standard deviation of the CV is computed across plant function types (PFTs) in each of the four tundra types (Table 1) for a given model input parameter, or set of parameters, as described in Table 2.

photosynthetic temperature (0.2) parameter groupings were the smallest.

Summary of model sensitivity and uncertainty across arctic tundra plant communities, plant functional types, and output variables

Across all sites, PFTs, and output variables, there were some parameters that consistently influenced model sensitivity and output uncertainty (Figs. 3, 4). Other parameters were rarely influential. The model was most sensitive to the parameters related to photosynthetic temperature (Fig. 4h), with modest contributions to sensitivity from the leaf area (Fig. 4e) and canopy conductance (Fig. 4g) parameters. For parameters related to the extinction coefficient (i.e., light harvesting; Fig. 4b), fine roots (Fig. 4c), and labile soil N (Fig. 4d), model sensitivity was generally low.

The fraction of model output uncertainty contributed by a given parameter was dominated primarily by parameters related to leaf area (Fig. 5e), photosynthetic temperature (Fig. 5h), and PPFD50 (Fig. 5i), where the fraction was between 0.9 and 1 in some instances (Fig.5e, h, i). However, in some cases, both the extinction coefficient (Fig. 5b) and fine-root parameter (Fig. 5c) groupings contributed significantly to model uncertainty. While Figs. 4 and 5 illustrate the generalities in sensitivity and uncertainty across the tundra types, PFTs, and output variables, we found important nuances when examining specific sites and output variables, which we discuss further below, highlighting key parameters and output variables of interest.

Site-level and PFT-level comparisons

Shrub tundra across the latitudinal transect and in the Seward Peninsula.—In shrub tundra, the model sensitivity (Fig. 6; Appendix S1: Fig. S2) and uncertainty (Fig. 7) varied by model output variable and PFT for both the Dalton Highway latitudinal transect and for the shrub tundra Kougarok site. For example, these dynamics were pronounced for the parameter grouping related to photosynthetic temperature when examining sensitivity of NPP for the dwarf birch shrubs. Furthermore, while the dwarf birch shrubs showed a high sensitivity to photosynthetic parameters, the NPP of the other deciduous shrubs in the shrub tundra was not sensitive to this parameter grouping (Fig. 6b), and were generally not sensitive to any of the parameters tested for the other output variables (R_H, Soil C, Veg C; Appendix S1: Fig. S2). For the parameters related to canopy conductance, the shrub tundra sites more consistently agreed across output variables and PFTs in exhibiting negative sensitivity (Fig. 6a, b, d, e).

Model uncertainty for shrub tundra was driven by all parameter groups. For example, for NPP of the dwarf birch shrubs, willow shrubs, and other deciduous shrubs,
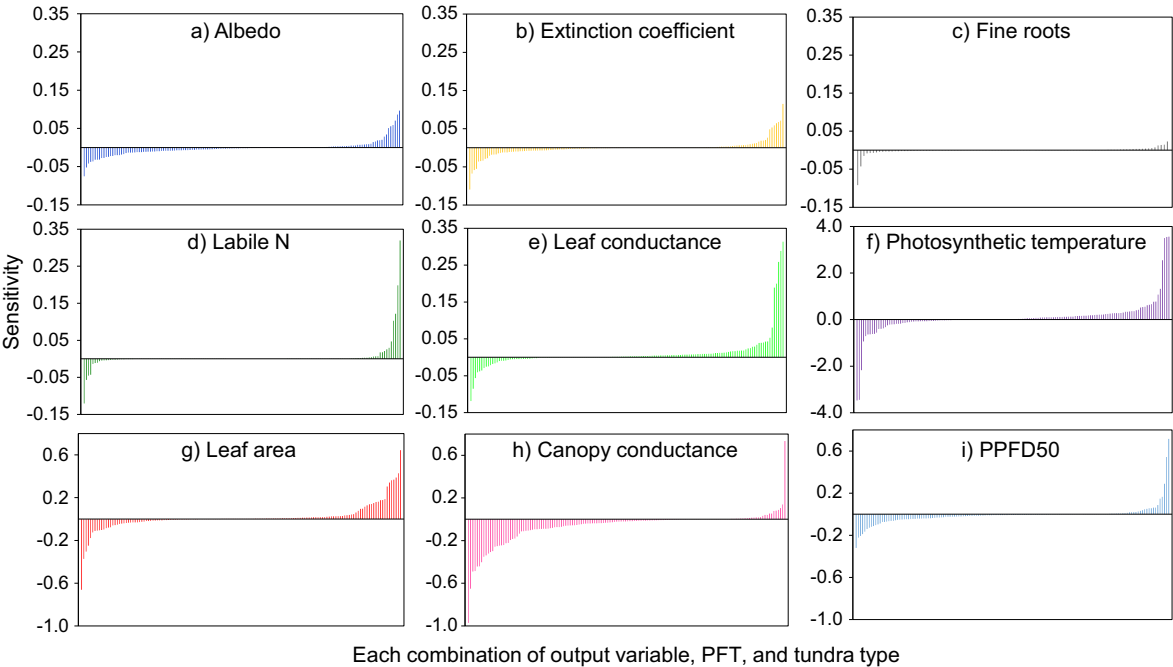
FIG. 4. Model sensitivity grouping all output variables analyzed (NPP, R_H, Veg C, Soil C) across the dominant plant functional types within four tundra types (Table 1) for a given grouping of parameters as defined in Table 2. Each bar on the graph represents one combination of output variable, PFT, and tundra type (Table 1), resulting in 144 values on each graph, except for fine roots with 100 values because mosses and lichens do not have roots. Note the three different y-axis scales when comparing across panels, with panels (a)–(e) ranging from −0.15 to 0.35, panel (f) ranging from −4.0 to 4.0, and panels (g)–(i) ranging from −1.0 to 0.8.
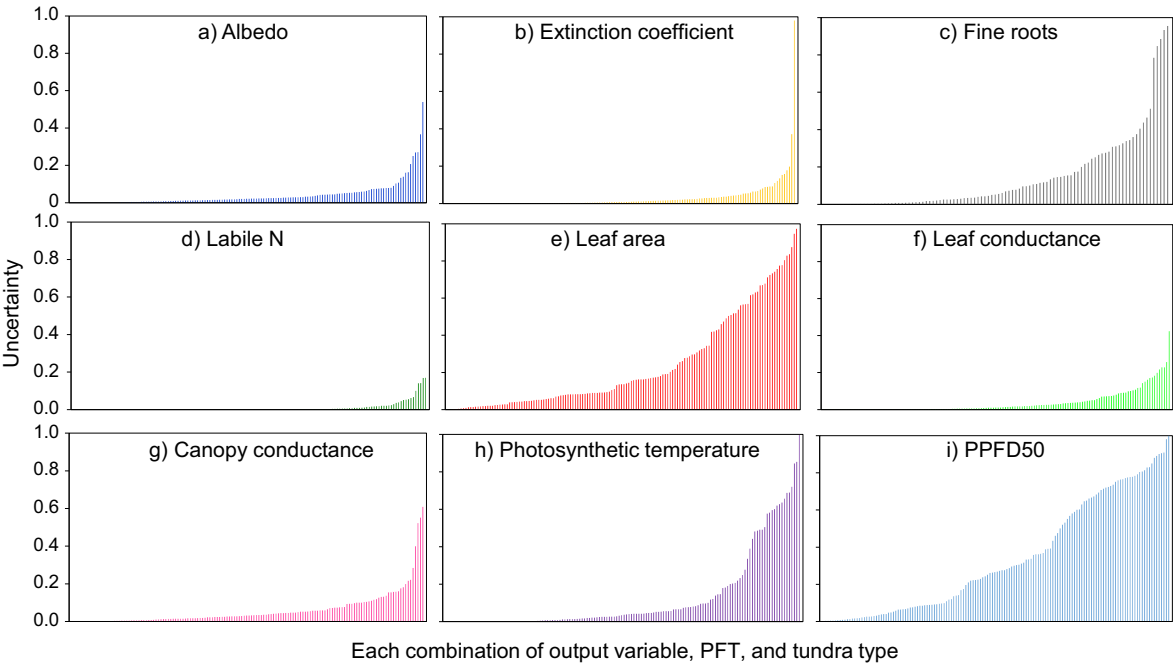

FIG. 5. Contribution of groupings of parameters (Table 2) to model uncertainty, grouping all output variables analyzed (NPP, R_H, Veg C, Soil C; Table 3) across the dominant plant functional types within four tundra types (Table 1). Each bar on the graph represents on combination of output variable, PFT, and tundra type, resulting in 144 observations on each graph, except for fine roots with 100 observations because mosses and lichens do not have roots.

the parameter related to the radiation influence on stomatal closure, PPFD50, showed the greatest contribution to model uncertainty, although the parameters related to the fine roots and canopy conductance were also influential (Fig. 7a–c). For the feathermoss in the shrub tundra, the leaf area parameters were consistently the greatest contribution to model uncertainty (Fig. 7d, h, l, p). Overall, in the shrub tundra Kougarok site, a wider range of parameters typically contributed to model uncertainty compared to the shrub tundra sites along the transect (Fig. 7e, h, i).

Seward Peninsula: Tussock tundra, heath tundra, shrub tundra.—Given that we observed PFTs within the shrub tundra (i.e., dwarf birch shrubs, willow shrubs, other deciduous shrubs, and feathermoss) along the transect and in the shrub tundra Kougarok site that showed differences in model sensitivity and uncertainty, we examined tundra communities located in close proximity (~≤0.5 km apart) at the Kougarok site. These included heath tundra, tussock tundra, and shrub tundra. Our analysis includes tundra communities that contain some of the same PFTs (Table 1). For example, dwarf birch shrubs are in both the shrub tundra and tussock tundra, and evergreen shrubs are in both the heath tundra and tussock tundra, while moss is found in all three tundra communities (Table 1, Fig. 8).

In terms of model sensitivity, we found that the same PFT, located in different tundra communities, but under the same climate, could have opposite responses, using

the photosynthetic temperature parameter grouping as an example (Fig. 8a–d). In the dwarf birch for the Soil C output, the sensitivity to photosynthetic temperature was −0.7 for dwarf birch in the shrub tundra, and 0.2 for dwarf birch in the tussock tundra (Fig. 8c). Moss was prevalent in all three tundra types, and the model outputs were generally not sensitive to the photosynthetic temperature parameters, except for R_H in the shrub tundra and tussock tundra (Fig. 8a–d).

We also found key differences in model uncertainty for the same PFTs in different tundra communities. For example, this was pronounced with dwarf birch $\underline{R}_H$ in the shrub tundra and tussock tundra, where the greatest contribution to model uncertainty in the shrub tundra was the canopy conductance parameter, but was the PPFD50 parameter in the tussock tundra (Fig. 8f). However, overall, there were some parameters across the tundra communities and PFTs that consistently influenced model uncertainty, including PPFD50, photosynthetic temperature, and LAI.

Utqiagvik.—The sedges, grasses, feathermoss, and *Sphagnum* in the wet sedge tundra near Utqiagvik showed sensitivity to a wide range of model parameters for the output variables R_H and Vegetation C (Fig. 9b,d). However, for the NPP and Soil C outputs the model showed low sensitivity to the parameters, except for the NPP of the sedges (Fig. 9a,c).

The model uncertainty in the wet sedge tundra was primarily due to the parameters related to photosynthetic temperature across all model outputs and PFTs,
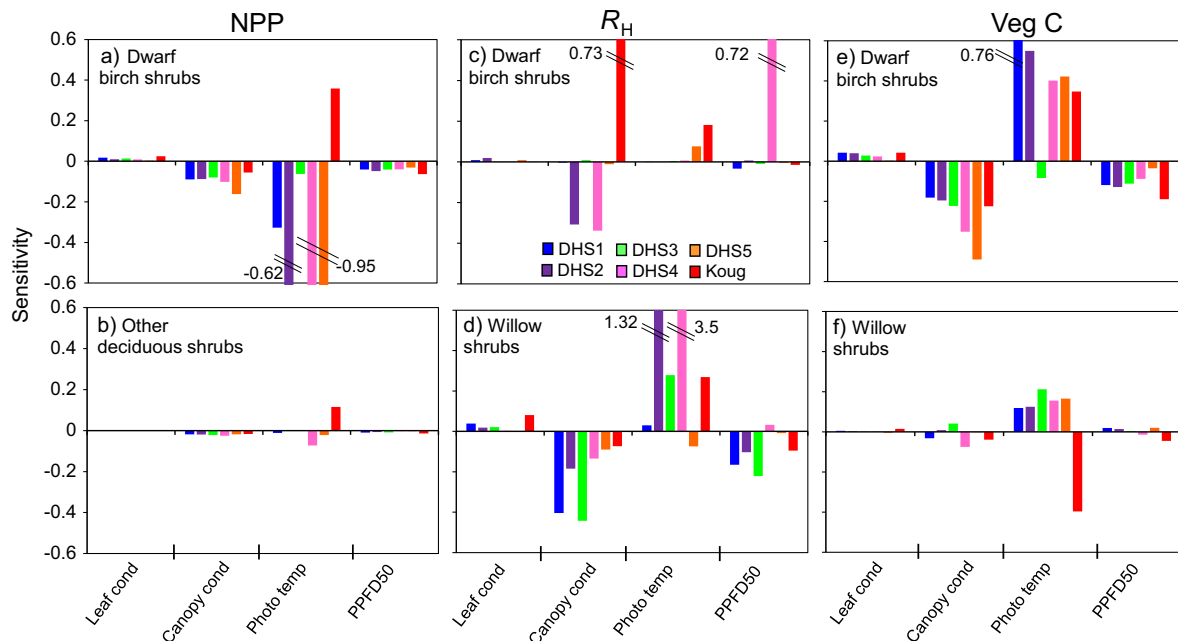

FIG. 6. Model sensitivity in the shrub tundra sites for selected parameters. DHS is the Dalton Highway Site, with DHS1 as the site furthest south and DHS5 the site furthest north on the transect. "Koug" refers to the shrub tundra at the Kougarok site. No error bars are shown because the standard deviation within each parameter grouping was small (~0.01).
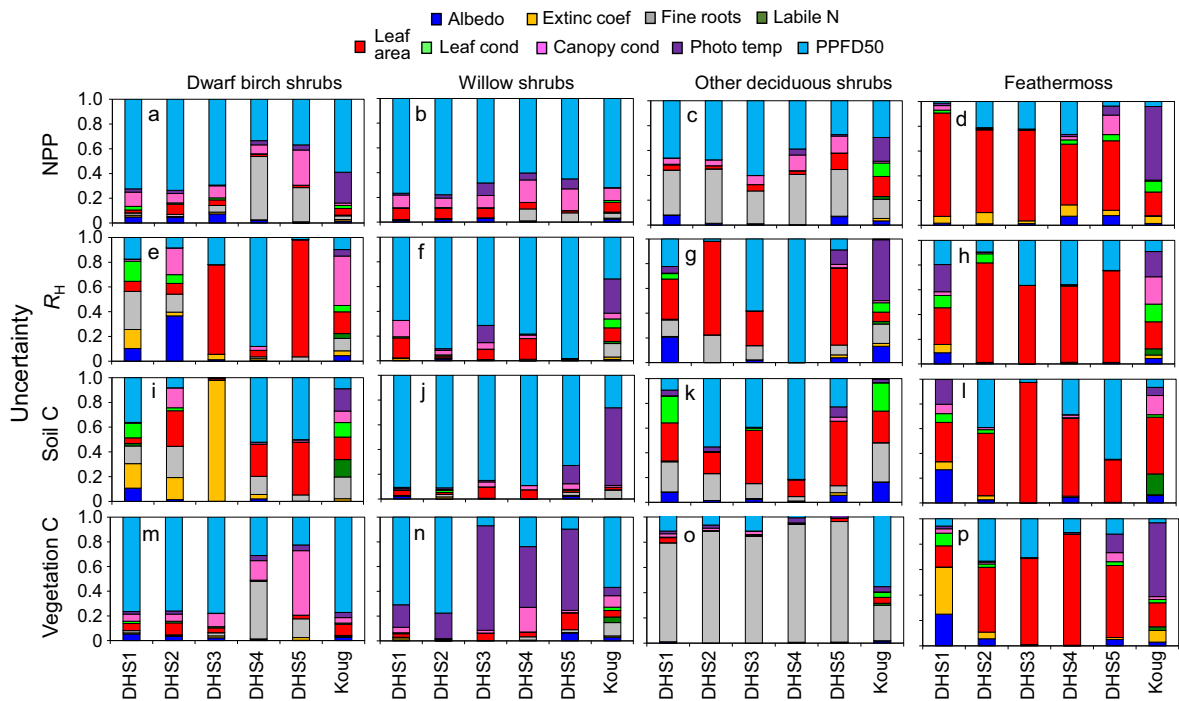
FIG. 7. Model uncertainty in the shrub tundra. DHS is the Dalton Highway Site, with DHS1 as the site furthest south and DHS5 the site furthest north on the transect. "Koug" refers to the shrub tundra at the Kougarok site.
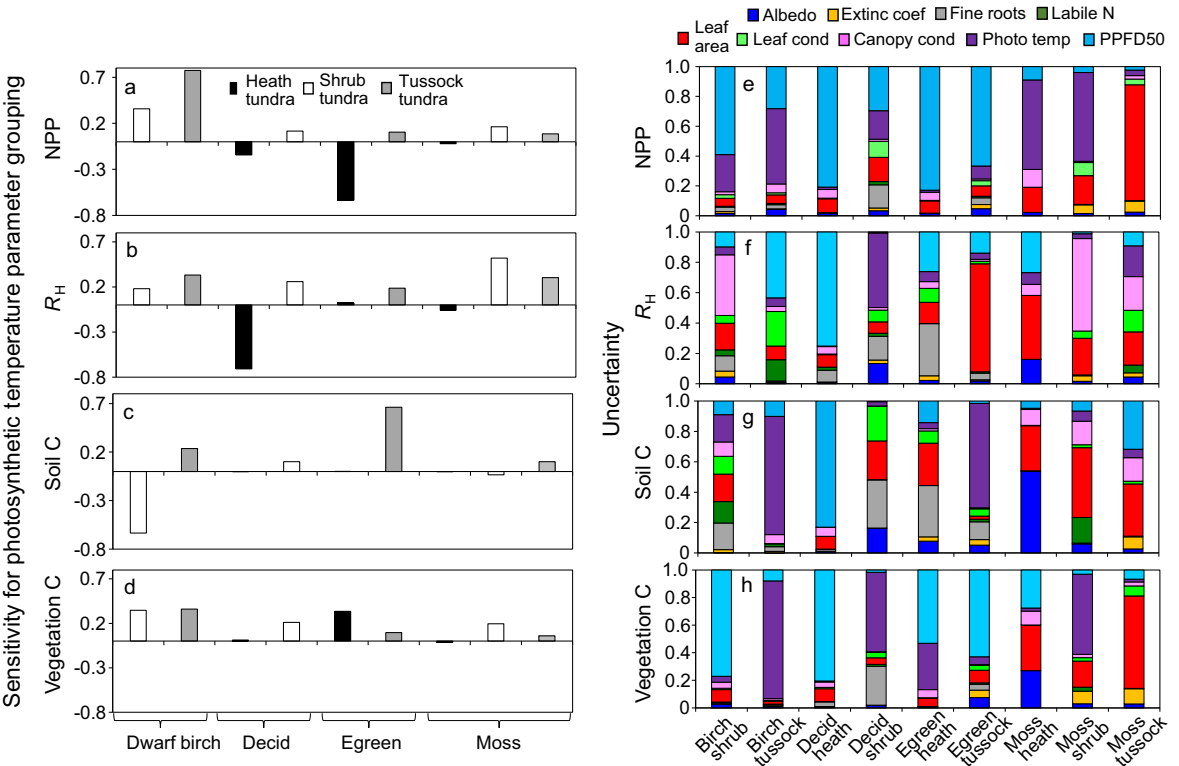

FIG. 8. (a–d) Model sensitivity for selected parameter groupings and (e–h) uncertainty across heath, tussock, and shrub tundra types located in close proximity to each other at the Kougarok site. No error bars are shown because the standard deviation within each parameter grouping was small (~0.01).

except for the sedges (Fig. 9e–h). The model uncertainty in the sedges was distributed across numerous parameter groupings. The parameters related to fine roots were influential for the R_H and Soil C of the grasses and sedges.

Uncertainty in pools and fluxes from 1990 to 2015.—The estimated model uncertainty due to the selected input parameters (Table 2) allowed us to quantify ranges of the model outputs, or response variables, in this case NPP, R_H, Soil C, and Vegetation C at the plant community level (shrub tundra, tussock tundra, heath tundra, wet sedge tundra; Table 3). Based on the ensemble of model simulations, we calculated 25th and 75th quantiles of the outputs. For NPP in the shrub tundra, the 25th quantile resulted in NPP values between 13% and 17% lower, and the 75th quantile resulted in values 14–18% higher. In the wet sedge tundra, the quantiles were greater, at 23% and 36% for the 25th and 75th quantiles, respectively. Overall, the values of NPP varied from 99 g C·m^{-2}·yr^{-1} in the heath tundra to 671 g C·m^{-2}·yr^{-1} in the wet sedge tundra. For the flux R_H, pulses of respiration resulted in estimates in the 75th percentile between 23% and 49% higher in the shrub tundra. R_H showed less variability across the sites than NPP, ranging from 211 g C·m^{-2}·yr^{-1} in the heat tundra to 351 g C·m^{-2}·yr^{-1} in the tussock tundra. The pool of soil carbon showed large variability in the quantiles across

tundra types, ranging from just 1% in the heath tundra to 23% at one shrub tundra site. The pool of soil C was smallest in the heath tundra at 18 kg C/m^2 to 44 g C/m^2 in the shrub tundra at the Kougarok site. For vegetation C, the 25th percentile ranged from 11% in the heath tundra to 28% in the wet sedge tundra, and the 75th percentile ranged from 12% in the heath tundra to 29% at one of the shrub tundra sites. Vegetation C ranged from 298 g C·m^{-2}·yr^{-1} at the heath tundra site to 1,283 at the wet sedge tundra. These results suggest that error in the model outputs due to input parameter uncertainty varies geographically within one community type (shrub tundra) and also across community types, with heath tundra generally showing the smallest uncertainty and wet sedge tundra the greatest.

Discussion

Uncertainty in high-latitude ecosystem biogeochemistry models contributes to a large spread in simulations of key response variables that determine the trajectory of these sensitive ecosystems under a changing climate (Fisher et al. 2014, McGuire et al. 2018). Here, we assessed one aspect of this uncertainty, parameter uncertainty, for one model developed specifically for arctic and boreal ecosystems, the Terrestrial Ecosystem Model with Dynamic Vegetation and Dynamic Organic Soil Layers, newly integrated into the PEcAn
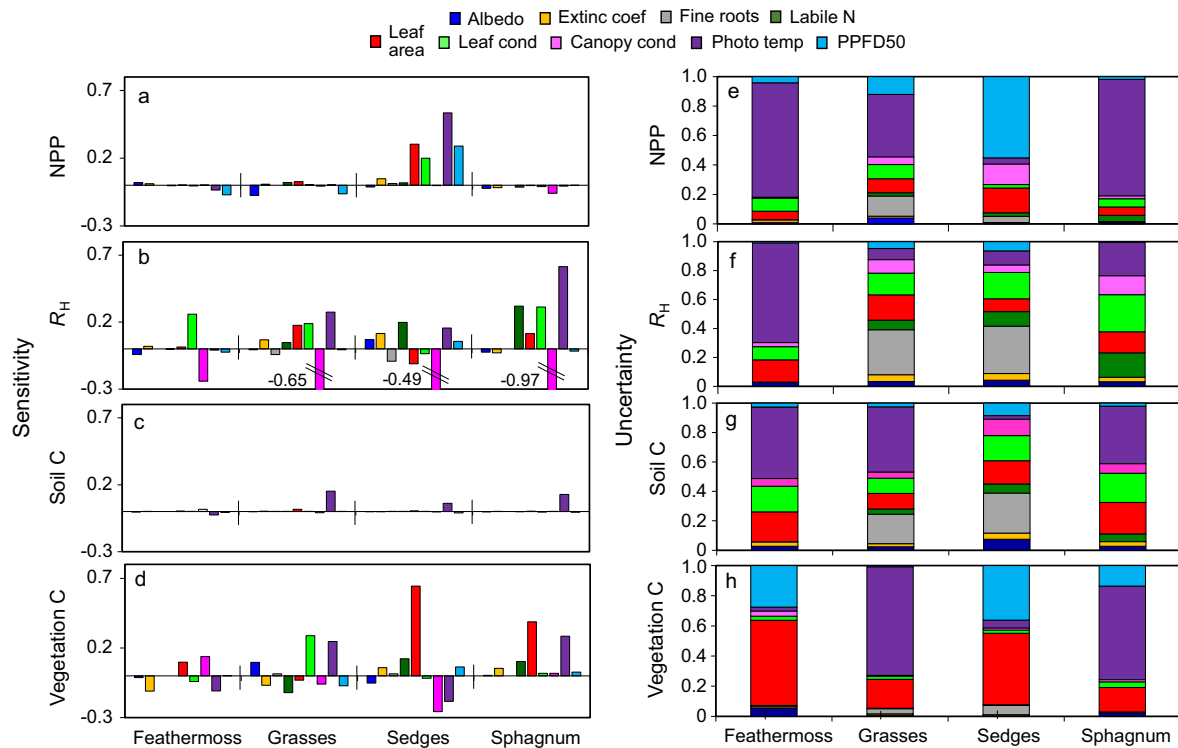

FIG. 9. (a–d) Model sensitivity and (e–h) uncertainty in wet sedge tundra at Utqiagvik, Alaska. No error bars are shown because the standard deviation within each parameter grouping was small (~0.01).

TABLE 3. Median values and quantiles of pools and fluxes for 1990–2015.

Site	NPP (g C·m^{-2}·yr^{-1})	Difference for a quantile (%)		R_H (g C·m^{-2}·yr^{-1})	Difference for a quantile (%)		Soil C (kg C/m^2)	Difference for a quantile (%)		Veg C (g C/m^2)	Difference for a quantile (%)	
		25th	75th		25th	75th		25th	75th		25th	75th
Dalton Highway shrub transect												
1	424	13	14	311	17	42	26	7	11	1,209	13	13
2	384	17	16	298	14	49	30	19	13	1,083	18	18
3	365	18	19	289	12	31	35	23	6	1,044	17	17
4	300	17	19	279	12	28	33	14	14	740	18	27
5	302	18	22	277	15	25	31	16	15	740	17	29
Kougarok												
Shrub	308	17	18	286	15	23	44	5	9	741	18	27
Tussock	671	17	18	351	6	8	38	12	3	957	18	20
Heath	99	20	21	211	2	4	18	1	1	298	11	12
Utqiagvik												
Wet sedge	115	23	36	212	3	32	30	2	4	1,283	28	25
Mean across quantiles		18	20		11	27		11	8		18	21

Notes: NPP, net primary productivity; R_H, heterotrophic respiration; Veg C, vegetation C.

framework. Given the large uncertainty in the arctic carbon cycle, including whether the Arctic is a CO_2 sink, source, or approximately in balance (McGuire et al. 2012, Belshe et al. 2013, Fisher et al. 2014), we examined four response variables related to carbon cycling (NPP, R_H, Soil C, and Vegetation C). Our work here is a first step towards gaining this understanding within the context of the TEM-PEcAn framework. Additional inquiry is currently underway using this framework to examine these dynamics going forward, including assessing how parameters may covary and performing model projections into the future to 2100 to examine the net carbon balance. In our discussion below, we consider aspects of our analysis that are unique to arctic tundra plant communities and additional steps to take going forward.

Uncertainty in high latitudes

Arctic tundra landscapes are highly heterogeneous due to small-scale variations in permafrost conditions, vegetation composition, soil types, and moisture status. The North Slope of Alaska has been mapped to 24 terrestrial ecosystem communities, with greater detail than the broader tundra types we include in our study, including several types of tussock tundra, shrub tundra, heath tundra, and wet sedge tundra (Jorgenson and Heiner 2003). This landscape heterogeneity is the determining factor of variability in the regional carbon balance of tundra ecosystems (Zulueta et al. 2011, Treat et al. 2018). Consequently, given that each of these tundra types, and the PFTs contained within them, could be parameterized differently in an ecosystem model, it is important to examine how the sensitivity and uncertainty vary across the PFTs in various tundra types. Here, we found a wide range of parameters driving GPP, to which TEM was sensitive and which influenced model

uncertainty across four types of tundra, although a few parameters were more prominent, including those related to photosynthetic temperature, leaf area, and canopy conductance for model sensitivity (Fig. 4). For uncertainty, the model was largely influenced by parameters related to leaf area, photosynthetic temperature, and the stomatal response to light (Fig. 5). Our results also illustrate even further complexity, with geographical differences in sensitivity and uncertainty even within the same community type, such as shrub tundra (Figs. 5, 6). The geographical differences within one community type (i.e., shrub tundra) across an environmental gradient suggests that there may be phenotypic variation or an interaction between the environment and vegetation that is governing this variation in the parameter sensitivity or uncertainty. Furthermore, this finding suggests that model parameterization may need to move away from one parameterization for a species or PFT to include other environmental interactions associated with the parameters, and could involve separate model calibrations for each site. This type of model parameterization and calibration that considers phenotypic variation or environmental interactions would be applicable not just in arctic tundra but also in other biomes. However, the implementation of these types of parameterizations and calibrations would need to be assessed carefully. This could be done by performing the type of parameter sensitivity and uncertainty study we present here to first determine which parameters influence model sensitivity and uncertainty the most given that this additional detail in the parameters would likely be both time-consuming to collect and computationally expensive to implement in the model.

Model parameter sensitivity and uncertainty caused variation in the overall ranges in the response variables in terms of the values of NPP, R_H, Soil C, and Vegetation C from 1990 to 2015 across sites (Table 3),

illustrating challenges in constraining the C budget in these tundra ecosystems. The large variability in the Soil C and R_H are particularly relevant in the context of a thawing permafrost landscape and potential C emissions (Schuur et al. 2015). Likewise, as we work towards gaining a better understanding of tundra plant productivity under a warming climate (Myers-Smith et al. 2011, 2015), the model uncertainty related to NPP and Vegetation C are relevant.

Studies examining model parameter sensitivity and uncertainty in the context of arctic ecosystem biogeochemistry models are rare. Davidson (2012) applied the Ecosystem Demography (ED2) model and the PEcAn framework to tundra in northern Alaska and found that the parameters that contributed the most to model uncertainty in selected response variables (aboveground biomass, diameter growth, and net ecosystem exchange) included reproductive allocation, growth respiration, and leaf allometry. Fine-root allocation parameters also had some influence on model uncertainty in certain PFTs in ED2, similar to our findings. Dietze et al. (2014) examined the NPP response across a wide range of biomes and PFTs also using ED2 within the PEcAn framework, hypothesizing that the importance of temperature-limited parameters would increase with latitude. However, in both Davidson (2012) and Dietze et al. (2014), a parameter related to photosynthetic temperature had no effect in tundra, which differs from our findings. This may be related to differences in the functional forms of the model and, in particular, for the equation underlying the calculation of GPP. That is, different methods of calculating GPP across models may result in differences in our interpretation of model parameter uncertainty and sensitivity. These results suggest the value of performing a multi-model intercomparison of sensitivity and uncertainty across TBMs simulated at tundra sites to determine if there is a set of parameters that consistently influence model sensitivity and uncertainty. This type of model intercomparison would then permit the separation of parameter uncertainties and sensitivity across models from differences in model structural uncertainties. This would then help to formulate data needs that are common across models to those that are linked simply to the structure of a specific model and could be applied to other regions than the arctic tundra.

Future data collection

The Arctic has long been considered data sparse due to its cold climate and remote geography. A recent study found that data acquisition in the terrestrial arctic is primarily concentrated near roads, populations, or field stations (Metcalfe et al. 2018), and this is certainly true in northern Alaska. Long-term monitoring programs and experiments are also rare. Furthermore, many types of data collection in terrestrial arctic ecosystems require easy access to a laboratory setting for further sample processing, and in remote arctic settings, laboratory space is limited or nonexistent. Consequently, arctic ecosystem models often lack data for parameterization, substituting model parameters for arctic ecosystems with those from lower latitudes, especially when the model was initially developed for temperate regions (Davidson 2012). Thus, for the parameters that are recognized as influential on model uncertainty, how difficult are the data to collect in the Arctic?

Parameters related to leaf area, including LAI and SLA, are relatively easy to collect across tundra communities and PFTs. Others, such as those related to optimal photosynthetic temperature parameters require the construction of temperature response curves (Rogers et al. 2017) that typically take place in a laboratory setting immediately following plant data collection in the field. The fine-root parameters are also laborious to measure, especially with the need to distinguish the roots across plants species, at multiple depth increments, and in permafrost soils (Iversen et al. 2015). Biomass harvests of plant tundra communities to determine allocation between the wood, leaf, and root components are labor intensive and need to be performed within the narrow window of peak biomass in late July. Consequently, when determining which data to collect in the field, it is important to consider for which parameters even a small amount of data constraint will likely prove effective in reducing predictive uncertainty.

Recent advances in remote sensing and multi-sensor data from unoccupied aerial systems (UASs) of plant traits may also prove key in improving parameterization of arctic ecosystem models (Schimel et al. 2015, Yang et al. 2020). The LAI of arctic PFTs can be estimated using active LiDAR (Magney et al. 2016) and through optical multispectral imagery (Juutinen et al. 2017). Leaf economic traits including leaf N and SLA are detectable using leaf to landscape hyperspectral remote sensing (Smith et al. 2002, Singh et al. 2015, Serbin et al. 2019). Other recent efforts with a newly developed UAS deployed near the Seward Peninsula study site in this study have accurately mapped the tundra ecosystems, and measured canopy-scale greenness, canopy height, and other derived characteristics, such as shrub fraction and lichen fraction (Yang et al. 2020). Entirely indirect traits such as root characteristics may seem impossible to measure with remote sensing (given that remote sensing struggles to penetrate most soil types) but mapping root traits will become tractable by identifying covarying aboveground (i.e., leaf and size traits) and belowground trait–trait relationships (Sloan et al. 2013). These methods of determining plant traits with remotely sensed and UAS data can take place across space and time, thereby potentially permitting the input of spatially, and even temporally, explicit maps of plant traits into arctic ecosystem models, considering variation in parameters across a geographic area (e.g., the phenotypic plasticity idea as discussed above), thereby helping to reduce model parameter uncertainty.

Mechanics in the PEcAn set-up

When performing the initial set-up within the PEcAn framework, there are considerations to take into account that could have an impact on the results, including the time period over which the response variables are analyzed, and the input parameter distributions. Here, we analyzed the simulations from the period 1990–2015. While it is possible that there could be an effect of simulation time period (e.g., 1 yr vs. 10 yr vs. decades) on the model uncertainty, this has not been observed in other studies that have used this framework over a multiyear period (Dietze et al. 2014, Raczka et al. 2018). The model input parameter distributions we used were based on expert and literature-based estimates. Given that these distributions can have a large impact on model sensitivity, as more data become available, it will be beneficial to reassess their accuracy.

CONCLUSION

The framework presented here provides an in-depth and reproducible parameter sensitivity and uncertainty analysis for ecosystems in the Arctic and elsewhere. We find that sensitivity and uncertainty related to model parameters in the heterogeneous arctic landscape is complicated. It is necessary to assess this uncertainty across a range of tundra types and the plant functional types within them for several response variables. The parameters do not necessarily contribute equally to model sensitivity or uncertainty within the same community type over an environmental gradient, such as the shrub tundra sites we analyzed. Even the model sensitivity and uncertainty in tundra types within close proximity and including some similar PFTs could vary widely. The analysis we present here is simply an initial step in accounting for and reducing uncertainty in arctic ecosystem models. The next step will consider the parameters shown here to result in the greatest uncertainty and direct data collection efforts accordingly to provide additional model constraint. Even though parameter uncertainty is simply one source of model error, it typically accounts for much of the observed differences across ecosystem biogeochemistry models (Dietze et al. 2011), and is important to consider in projecting Arctic carbon budgets.

LITERATURE CITED

Belshe, E. F., E. A. G. Schuur, and B. M. Bolker. 2013. Tundra ecosystems observed to be CO_2 sources due to differential amplification of the carbon cycle. Ecology Letters 16:1307–1315.

Bhatt, U. S., D. A. Walker, M. K. Raynolds, P. A. Bieniek, H. E. Epstein, J. C. Comiso, J. E. Pinzon, C. J. Tucker, and I. V. Polyakov. 2013. Recent declines in warming and vegetation greening trends over Pan-Arctic tundra. Remote Sensing 5:4229–4254.

Box, J. E., et al. 2019. Key indicators of Arctic climate change: 1971–2017. Environmental Research Letters 14:045010.

Bradford, M. A., W. R. Wieder, G. B. Bonan, N. Fierer, P. A. Raymond, and T. W. Crowther. 2016. Managing uncertainty in soil carbon feedbacks to climate change. Nature Climate Change 6:751–758.

Chen, W., K. D. Tape, E. S. Euskirchen, S. Liang, A. Matos, J. Greenberg, and J. M. Fraterrigo. 2020. Impacts of arctic shrubs on root traits and belowground nutrient cycles across a Northern Alaskan climate gradient. Frontiers in Plant Science 11:588098. https://doi.org/10.3389/fpls.2020.588098

Clein, J. S., A. D. McGuire, E. S. Euskirchen, and M. P. Calef. 2007. The effects of different climate input data sets on simulated carbon dynamics in the western Arctic. Earth Interactions 11:1–24.

Cowtan, K., and R. G. Way. 2014. Coverage bias in the Had-CRUT4 temperature series and its impact on recent temperature trends. Quarterly Journal of the Royal Meteorological Society 140:1935–1944.

Davidson, C. D. 2012. The modeled effects of fire on carbon balance and vegetation abundance in Alaskan tundra. University of Illinois, Urbana-Champaign, Champaign, Illinois, USA.

Dietze, M. C., et al. 2011. Characterizing the performance of ecosystem models across time scales: a spectral analysis of the North American Carbon Program site-level synthesis. Journal of Geophysical Research 116:G04029.

Dietze, M. C., et al. 2014. A quantitative assessment of a terrestrial biosphere models data needs across North American biomes. Journal of Geophysical Research: Biogeosciences 119:286–300.

Dietze, M. C., D. S. LeBauer, and R. Kooper. 2013. On improving the communication between models and data. Plant, Cell, & Environment 36:1575–1585.

Dodd, E., C. J. Merchant, N. A. Rayner, and C. P. Morice. 2015. An investigation into the impact of using various techniques to estimate Arctic surface air temperature anomalies. Journal of Climate 28:1743–1763.

Euskirchen, E. S., et al. 2006. Importance of recent shifts in soil thermal dynamics on growing season length, productivity, and carbon sequestration in terrestrial high-latitude ecosystems. Global Change Biology 12:1–20.

Euskirchen, E. S., A. Bennett, A. L. Breen, H. Genet, M. Lindgren, T. Kurkowski, A. D. Mcuire, and T. S. Rupp. 2016. Consequences of changes in vegetation and snow cover for climate feedbacks in Alaska and northwest Canada. Environmental Research Letters 11:105003.

Euskirchen, E. S., M. S. Bret-Harte, G. J. Scott, C. Edgar, and G. R. Shaver. 2012. Seasonal patterns of carbon dioxide and water fluxes in three representative tundra ecosystems in northern Alaska. Ecosphere 3:1–19.

Euskirchen, E. S., T. B. Carman, and A. D. McGuire. 2014. Changes in structure and function of northern Alaskan ecosystems when considering variable leaf-out times across groupings of species in a dynamic vegetation model. Global Change Biology 20:963–978.

Euskirchen, E. S., A. D. McGuire, and F. S. Chapin III. 2007. Energy feedbacks to terrestrial ecosystems due to reduced high-latitude snow cover during 20th century warming. Global Change Biology 13:2425–2438.

Euskirchen, E. S., A. D. McGuire, F. S. Chapin III, S. Yi, and C. C. Thompson. 2009. Changes in vegetation in northern Alaska under scenarios of climate change, 2003–2100: implications for climate feedbacks. Ecological Applications 19:1022–1043.

Fisher, J. B., et al. 2014. Carbon cycle uncertainty in the Alaskan Arctic. Biogeosciences 11:4271–4288.

Fisher, J. B., et al. 2018. Missing pieces to modeling the Arctic-Boreal puzzle. Environmental Research Letters 13:020202.

Genet, H., et al. 2018. The role of driving factors in historical and projected carbon dynamics of upland ecosystems in Alaska. Ecological Applications 28:5–27.

Gough, L., J. C. Moore, G. R. Shaver, R. T. Simpson, and D. R. Johnson. 2012. Above- and belowground responses of arctic tundra ecosystems to altered soil nutrients and mammalian herbivory. Ecology 93:1683–1694.

Hararuk, O., M. J. Smith, and Y. Luo. 2015. Microbial models with data-driven parameters predict stronger soil carbon responses to climate change. Global Change Biology 21:2439–2453.

Harris, I., P. D. Jones, T. J. Osborn, and D. H. Lister. 2014. Updated high-resolution grids of monthly climatic observations – the CRU TS3.10 dataset. International Journal of Climatology 34:623–642.

Hugelius, G., et al. 2014. Estimated stocks of circumpolar permafrost carbon with quantified uncertainty ranges and identified data gaps. Biogeosciences 11:6573–6593.

Iversen, C. M., V. L. Sloan, P. F. Sullivan, E. S. Euskirchen, A. D. McGuire, R. J. Norby, A. P. Walker, J. M. Warren, and S. D. Wullschleger. 2015. The unseen iceberg: plant roots in arctic tundra. New Phytologist 205:34–58.

Jorgenson, M. T., and M. Heiner. 2003. Ecosystems of northern Alaska. 1:2.5 million-scale map produced by ABR, Inc., Fairbanks, Alaska, USA and The Nature Conservancy, Anchorage, Alaska, USA.

Juutinen, S., T. Virtanen, V. Kondratyev, T. Laurila, M. Linkosalmi, J. Mikola, J. Nyman, A. Räsänen, J.-P. Tuovinen, and M. Aurela. 2017. Spatial variation and seasonal dynamics of leaf-area index in the arctic tundra: implications for linking ground observations and satellite images. Environmental Research Letters 12:095002.

Keenan, T. F., and W. J. Riley. 2018. Greening of the land surface in the world's cold regions consistent with recent warming. Nature Climate Change 8:825–828.

Langford, Z. L., J. Kumar, F. M. Hoffman, A. L. Breen, and C. M. Iversen. 2019. Arctic vegetation mapping using unsupervised training datasets and convolutional neural networks. Remote Sensing 11:69.

Langford, Z., J. Kumar, F. M. Hoffman, R. J. Norby, S. D. Wullschleger, V. L. Sloan, and C. M. Iversen. 2016. Mapping Arctic plant functional type distributions in the Barrow Environmental Observatory using WorldView-2 and LiDAR datasets. Remote Sensing 8:733.

Lara, M. J., I. Nitze, G. Grosse, P. Martin, and A. D. McGuire. 2018. Reduced arctic tundra productivity linked with landform and climate change interactions. Scientific Reports 8:2345.

LeBauer, D. S., D. Wang, K. Richter, C. Davidson, and M. C. Dietze. 2013. Facilitating feedbacks between field measurements and ecosystem models. Ecological Monographs 83:133–154.

Lique, C., M. M. Holland, Y. B. Dibike, D. M. Lawrence, and J. A. Screen. 2016. Modeling the Arctic freshwater system and its integration in the global system: lessons learned and future challenges. Journal of Geophysical Research: Biogeosciences 121:540–566.

López-Blanco, E., M. Lund, T. R. Christensen, M. P. Tamstorf, T. L. Smallman, D. Slevin, A. Westergaard-Nielsen, B. U. Hansen, J. Abermann, and M. Williams. 2018. Plant traits are key determinants in buffering the meteorological sensitivity of net carbon exchanges of Arctic tundra. Journal of Geophysical Research: Biogeosciences 123:2675–2694.

Lovenduski, N. S., and G. B. Bonan. 2017. Reducing uncertainty in projections of terrestrial carbon uptake. Environmental Research Letters 12:101001.

Magney, T. S., et al. 2016. LiDAR canopy radiation model reveals patterns of photosynthetic partitioning in an Arctic shrub. Agricultural and Forest Meteorology 221:78–93.

McGuire, A. D., et al. 2012. An assessment of the carbon balance of Arctic tundra: comparisons among observations, process models, and atmospheric inversions. Biogeosciences 9:3185–3204.

McGuire, A. D., et al. 2018. Dependence of the evolution of carbon dynamics in the northern permafrost region on the trajectory of climate change. Proceedings of the National Academy of Sciences USA 115:3882–3887.

McGuire, A. D., J. M. Melillo, L. A. Joyce, D. W. Kicklighter, A. L. Grace, B. Moore, and C. J. Vorosmarty. 1992. Interactions between carbon and nitrogen dynamics in estimating net primary productivity for potential vegetation in North America. Global Biogeochemical Cycles 6:101–124.

Mekonnen, Z. A., W. J. Riley, and R. F. Grant. 2018. 21st century tundra shrubification could enhance net carbon uptake of North America Arctic tundra under an RCP8.5 climate trajectory. Environmental Research Letters 13:054029.

Metcalfe, D. B., et al. 2018. Patchy field sampling biases understanding of climate change impacts across the Arctic. Nature Ecology and Evolution 2:1443–1448.

Myers-Smith, I. H., et al. 2011. Shrub expansion in tundra ecosystems: dynamics, impacts and research priorities. Environmental Research Letters 6:45509.

Myers-Smith, I. H., et al. 2015. Climate sensitivity of shrub growth across the tundra biome. Nature Climate Change 5:887–891.

Norby, R. J., V. L. Sloan, C. M. Iversen, and J. Childs. 2019. Controls on fine-scale spatial and temporal variability of plant-available inorganic nitrogen in a polygonal tundra landscape. Ecosystems 22:528–543.

Overland, J., E. Dunlea, J. E. Box, R. Corell, M. Forsius, V. Kattsov, M. S. Olsen, J. Pawlak, L.-O. Reiersen, and M. Wang. 2019. The urgency of Arctic change. Polar Science 21:6–13.

Park, T., S. Ganguly, H. Tømmervik, E. S. Euskirchen, K.-A. Høgda, S. R. Karlsen, V. Brovkin, R. R. Nemani, and R. B. Myneni. 2016. Changes in growing season duration and productivity of northern vegetation inferred from long-term remote sensing data. Environmental Research Letters 11:084001.

Phoenix, G. K., and J. W. Bjerke. 2016. Arctic browning: extreme events and trends reversing arctic greening. Global Change Biology 22:2960–2962.

Raczka, B., M. C. Dietze, S. P. Serbin, and K. J. Davis. 2018. What limits predictive certainty of long-term carbon uptake? Journal of Geophysical Research: Biogeosciences 123:3570–3588.

Raich, J. W., E. B. Rastetter, J. M. Melillo, D. W. Kicklighter, P. A. Steudler, B. J. Peterson, A. L. Grace, B. Moore III, and C. J. Vorosmarty. 1991. Potential net primary productivity in South America: application of a global model. Ecological Applications 1:399–429.

Rogers, A., S. P. Serbin, K. S. Ely, V. L. Sloan, and S. D. Wullschleger. 2017. Terrestrial biosphere models underestimate photosynthetic capacity and CO_2 assimilation in the Arctic. New Phytologist 216:1090–1103.

Salmon, V. G., A. L. Breen, J. Kumar, M. J. Lar, P. E. Thornton, S. D. Wullschleger, and C. M. Iversen. 2019. Alder distribution and expansion across a tundra hillslope: implications for local N cycling. Frontiers in Plant Science 10:1099.

Schimel, D., R. Pavlick, J. B. Fisher, G. P. Asner, S. Saatchi, P. Townsend, C. Miller, C. Frankenberg, K. Hibbard, and P. Cox. 2015. Observing terrestrial ecosystems and the carbon cycle from space. Global Change Biology 21:1762–1776.

Schuur, E. A. G., et al. 2015. Climate change and the permafrost carbon feedback. Nature 520:171–179.

Serbin, S. P., J. Wu, K. S. Ely, E. L. Kruger, P. A. Townsend, R. Meng, B. T. Wolfe, A. Chlus, Z. Wang, and A. Rogers. 2019. From the Arctic to the tropics: multibiome prediction of leaf mass per area using leaf reflectance. New Phytologist 224:1557–1568.

Shaver, G. R., and F. S. Chapin III. 1991. Production: biomass relationships and element cycling in contrasting arctic vegetation. Ecological Monographs 61:1–31.

Singh, A., S. P. Serbin, B. E. McNeil, C. C. Kingdon, and P. A. Townsend. 2015. Imaging spectroscopy algorithms for mapping canopy foliar chemical and morphological traits and their uncertainties. Ecological Applications 25:2180–2197.

Sistla, S. A., J. C. Moore, R. T. Simpson, L. Gough, G. R. Shaver, and J. P. Schimel. 2013. Long-term warming restructures Arctic tundra without changing net soil carbon storage. Nature 497:615–618.

Sloan, V. L., B. J. Fletcher, M. C. Press, M. Williams, and G. K. Phoenix. 2013. Leaf and fine root carbon stocks and turnover are coupled across Arctic ecosystems. Global Change Biology 19:3668–3676.

Smith, M.-L., S. V. Ollinger, M. E. Martin, J. D. Aber, R. A. Hallett, and C. L. Goodale. 2002. Direct estimation of aboveground forest productivity through hyperspectral remote sensing of canopy nitrogen. Ecological Applications 12:1286–1302.

Strauss, J., et al. 2017. Deep Yedoma permafrost: a synthesis of depositional characteristics and carbon vulnerability. Earth-Science Reviews 172:75–86.

Sturm, M., C. Racine, and K. Tape. 2001. Climate change. Increasing shrub abundance in the Arctic. Nature 411:546–547.

Sullivan, P. F., M. Sommerkorn, H. M. Rueth, K. J. Nadelhoffer, G. R. Shaver, and J. M. Welker. 2007. Climate and species affect fine root production with long-term fertilization in acidic tussock tundra near Toolik Lake, Alaska. Oecologia 153:643–652.

Thompson, C., J. Beringer, F. S. Chapin III, and A. D. McGuire. 2004. Structural complexity and land-surface energy exchange along a gradient from arctic tundra toboreal forest. Journal of Vegetation Science 15:397–406.

Thompson, C. D., A. D. McGuire, J. S. Clein, F. S. Chapin III, and J. Beringer. 2006. Net carbon exchange across the arctic tundra–boreal forest transition in Alaska 1981–2000. Mitigation and Adaptation Strategies for Global Change 31:61–91.

Tian, H., J. M. Melillo, D. W. Kicklighter, A. D. McGuire, and J. Helfrich. 1999. The sensitivity of terrestrial carbon storage to historical climate variability and atmospheric CO_2 in the United States. Tellus 51B:414–452.

Treat, C. C., et al. 2018. Tundra landscape heterogeneity, not interannual variability, controls the decadal regional carbon balance in the Western Russian Arctic. Global Change Biology 24:5188–5204.

Van Wijk, M. T., M. Williams, J. A. Laundre, and G. R. Shaver. 2003. Interannual variability of plant phenology in tussock tundra: modelling interactions of plant productivity, plant phenology, snowmelt and soil thaw. Global Change Biology 9:743–758.

Viskari, T., A. Shiklomanov, M. C. Dietze, and S. P. Serbin. 2019. The influence of canopy radiation parameter uncertainty on model projections of terrestrial carbon and energy cycling. PLoS One 14:e0216512.

Walker, D. A., et al. 2005. The circumpolar Arctic vegetation map. Journal of Vegetation Science 16:267–282.

Wang, D., D. S. LeBauer, and M. C. Dietze. 2013. Predicting yields of short-rotation hybrid poplar (*Populus* spp.) for the contiguous US through model-data synthesis. Ecological Applications 23:944–958.

Yang, D., R. Meng, B. D. Morrison, A. McMahon, W. Hantson, D. J. Hayes, A. L. Breen, V. G. Salmon, and S. P. Serbin. 2020. A multi-sensor unoccupied aerial system improves characterization of vegetation composition and canopy properties in the Arctic tundra. Remote Sensing 12:1–24.

Yi, S., A. D. McGuire, E. Kasischke, J. Harden, K. Manies, M. Mack, and M. Turetsky. 2010. A dynamic organic soil biogeochemical model for simulating the effects of wildfire on soil environmental conditions and carbon dynamics of black spruce forests. Journal of Geophysical Research: Biogeosciences 115:G04015.

Zhuang, Q., et al. 2003. Carbon cycling in extratropical terrestrial ecosystems of the Northern Hemisphere during the 20th century: a modeling analysis of the influences of soil thermal dynamics. Tellus 55b:751–777.

Zhuang, Q., V. E. Romanovsky, and A. D. McGuire. 2001. Incorporation of a permafrost model into a large-scale ecosystem model: evaluation of temporal and spatial scaling issues in simulating soil thermal dynamics. Journal of Geophysical Research: Atmospheres 106d:33649–33670.

Zulueta, R. C., W. C. Oechel, H. W. Loescher, W. T. Lawrence, and U. K. T. Paw. 2011. Aircraft-derived regional scale CO_2 fluxes from vegetated drained thaw-lake basins and interstitial tundra on the Arctic Coastal Plain of Alaska. Global Change Biology 17:2781–2802.

Supporting Information

Open Research